A novel primary human immunodeficiency due to deficiency in the WASP-interacting protein WIP

Gaetana Lanzi,[1] Daniele Moratto,[1] Donatella Vairo,[1] Stefania Masneri,[1] Ottavia Delmonte,[2] Tiziana Paganini,[1] Silvia Parolini,[3] Giovanna Tabellini,[3] Cinzia Mazza,[1] Gianfranco Savoldi,[1] Davide Montin,[2] Silvana Martino,[2] Pierangelo Tovo,[2] Itai M. Pessach,[4] Michel J. Massaad,[4] Narayanaswamy Ramesh,[4] Fulvio Porta,[6] Alessandro Plebani,[1] Luigi D. Notarangelo,[4,5] Raif S. Geha,[4] and Silvia Giliani[1]

[1]A. Nocivelli Institute for Molecular Medicine, Pediatric Clinic, University of Brescia, and Laboratory of Genetic Disease of Childhood, Spedali Civili, 25123 Brescia, Italy
[2]Department of Pediatrics, University of Turin, 10126 Turin, Italy
[3]Department of Biomedical Sciences and Biotechnologies, University of Brescia, 25123 Brescia, Italy
[4]Division of Immunology and [5]The Manton Center for Orphan Disease Research, Children's Hospital, Harvard Medical School, Boston, MA 02115
[6]Division of Hematology and Oncology, Spedali Civili, 25123 Brescia, Italy

A female offspring of consanguineous parents, showed features of Wiskott–Aldrich syndrome (WAS), including recurrent infections, eczema, thrombocytopenia, defective T cell proliferation and chemotaxis, and impaired natural killer cell function. Cells from this patient had undetectable WAS protein (WASP), but normal *WAS* sequence and messenger RNA levels. WASP interacting protein (WIP), which stabilizes WASP, was also undetectable. A homozygous c.1301C>G stop codon mutation was found in the *WIPF1* gene, which encodes WIP. Introduction of WIP into the patient's T cells restored WASP expression. These findings indicate that WIP deficiency should be suspected in patients with features of WAS in whom *WAS* sequence and mRNA levels are normal.

CORRESPONDENCE
Silvia Giliani:
giliani@med.unibs.it

Abbreviations used: CFSE, carboxyfluorescein succinimidyl ester; hWIP, human WIP; IP10, C-X-C motif chemokine immune protein-10; rIl-2, recombinant IL-2; WAS, Wiskott-Aldrich syndrome; WASP, WAS protein; WIP, WASP interacting protein.

The Wiskott-Aldrich syndrome (WAS OMIM 301000) is an X-linked disorder characterized by thrombocytopenia, eczema, and immunodeficiency (Thrasher and Burns, 2010). T lymphocytes from WAS patients fail to proliferate and secrete IL-2 in response to cross-linking of the TCR–CD3 complex. Moreover, they exhibit actin cytoskeletal defects illustrated by defective F-actin polymerization after TCR–CD3 cross-linking, reduced ability to spread upon contact with anti-CD3–coated surfaces, impaired chemotaxis in vitro, and poor homing in vivo to lymphoid organs (Thrasher and Burns, 2010). NK cell function and immune synapse formation with target cells is also impaired in WAS (Orange et al., 2002; Gismondi et al., 2004; Stabile et al., 2010).

In T lymphocytes, WASP is almost totally complexed with the WASP-interacting protein (WIP; de la Fuente et al., 2007). A major function of WIP is to stabilize WASP and prevent its degradation. WASP protein levels, but not mRNA levels, are severely reduced in T cells from WIP-deficient mice. Introduction of full-length WIP, but not of WIP that lacks the WASP binding domain, restores WASP levels in these cells (de la Fuente et al., 2007). We describe for the first time a patient who presented in early infancy with a phenotype of WAS who was found to have a homozygous mutation in the *WIPF1* gene, which encodes WIP.

RESULTS AND DISCUSSION

Clinical characteristics

The index patient was the second female child of consanguineous Moroccan parents. She was referred at 11 d of age with poor weight gain,

G. Lanzi and D. Moratto contributed equally to this paper.
R.S. Geha and S. Giliani contributed equally to this paper.

The Rockefeller University Press $30.00
J. Exp. Med. Vol. 209 No. 1 29-34
www.jem.org/cgi/doi/10.1084/jem.20110896

Supplemental Material can be found at:
http://jem.rupress.org/content/suppl/2012/01/05/jem.20110896.DC1.html

Published January 9, 2012

an eczematous rash, papulovesicular lesions on the scalp, and ulcerative lesions on the hard palate and tongue. A previous female sibling suffered from ulcerative and vesicular skin lesions and died of sepsis at 4 mo of age.

Laboratory findings included thrombocytopenia (59×10^3/μl platelets) with normal platelet volume and elevated levels of C reactive protein (10.3 mg/dl; Table S1). Blood and urine cultures were negative. Stool cultures revealed no pathogenic organisms. *S. epidermidis* and *K. pneumoniae* grew from the skin vesicular lesions. The patient developed respiratory distress and required oxygen supplementation. A tracheal aspirate was positive for respiratory syncytial virus by PCR. She was placed on wide-spectrum antibiotic therapy, fungal and viral prophylaxis, immunoglobulin replacement, and platelet and red cell transfusions as needed. She developed rotavirus enteritis at 2 mo of age, and acute hepatitis of unknown etiology at 3 mo of age. No clinical manifestations of autoimmunity or bleeding tendency were noted. Because of persistent deterioration, failure to gain weight, and poor T cell function, at the age of 4.5 mo she underwent unrelated cord blood transplantation. 16 mo after the procedure, she is alive and well with >98% of T cells, >98% of B cells, 94% of NK cells, 50% of monocytes, and 41% of granulocytes of donor origin. The oral ulcerations resolved after bone marrow transplant, suggesting that they were secondary to deficient immune function.

Immunological analysis

Analysis of peripheral blood revealed low percentages and numbers of $CD3^+$ cells (809 cells/μl), with $CD8^+$ cells more affected than $CD4^+$ cells (Fig. 1 A and Table S1). 90% of

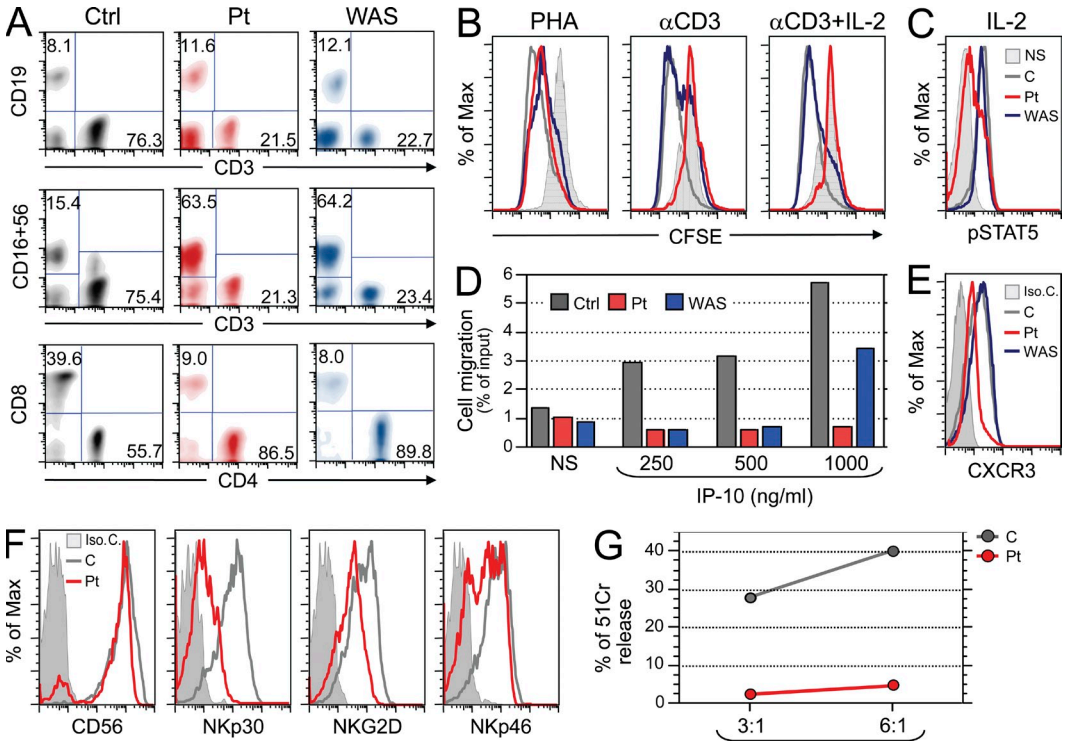

Figure 1. Functional characterization of WIP deficiency. (A) Evaluation of the proportion of T, B, and NK cells on gated lymphocytes in whole blood (top and middle row), and of CD4- and CD8-expressing cells on the $CD3^+$ gated cells (bottom row) of a control (Ctrl), the patient (Pt), and a WAS-null patient. Data are representative of three independent analyses. (B) T cell proliferation to PHA and anti-hCD3 with or without rIL-2, as assessed by CFSE dilution. PBMCs were used and FACS analysis was performed on $CD3^+$ gated cells. The solid gray histogram represents exemplificative profile of unstimulated cells. An overlapping profile was obtained from unstimulated cells of control and WAS patients (not depicted). The red, gray, and blue profiles represent CFSE content in stimulated cells from patient, control, and a WAS-null patient, respectively. Data are representative of two independent experiments. (C) PBMCs were stimulated with IL-2, and gated $CD3^+$ cells were analyzed by FACS for intracellular pSTAT5 using anti-pY^{694}STAT5. The solid line represents the signal in unstimulated patient's cells, which was comparable to that of unstimulated control and WAS-null patient cells (not depicted). The pSTAT5 signal in the rIL-2 stimulated cells from patient, control, and WAS patient are indicated in red, gray, and blue, respectively. Data are representative of three independent experiments. (D) Migration of PHA blasts from a healthy control, the patient and from a WAS-null patient toward the chemokine IP-10. The gray, red, and blue histograms represent migration of cells from control, patient, and WAS-null patient, respectively. Data are representative of two independent experiments. (E) Expression of the IP-10 receptor CXCR3 on PHA blasts from patient, control, and WAS-null patient. Isotype control staining of patient PHA blasts is shown by the filled histogram and was comparable to that of control T cells and WAS patient (not depicted). The CXCR3 signals in cells from patient, control, and WAS patient are indicated in red, gray, and blue, respectively. Data are representative of two independent experiments. (F) Expression of CD56, NKp30, NKGD2, and NKp46 on NK cells from patient (red) and control (gray). The filled histogram represents isotype control staining of patient NK cells, and was comparable to that of control NK cells (not depicted). Data are representative of two analyses. (G) Cytolytic activity by patient and control NK cell lines against the LCL 721.221 target cells, measured as the percentage of net ^{51}Cr release at effector (E) to target (T) ratios of 3:1 and 6:1. Data are representative of two independent experiments on the same expanded NK cells.

Published January 9, 2012

$CD3^+$ cells were $TCR\alpha\beta^+$, and 7% were $TCR\gamma\delta^+$. B cell number was low (319 cells/μL), whereas the percentage and number of $CD16^+CD56^+$ NK cells were increased (2,485 cells/μl; Fig. 1 A and Table S1), as reported in patients with WAS (Gismondi et al., 2004). Serum immunoglobulins were normal, except for elevated IgE (32 IU/ml).

Because of the clinical similarities between our patient and WAS patients we studied in parallel the function of her T cells and those from a WAS patient who expressed no detectable WASP protein. Analysis of T cell proliferation by CFSE dilution revealed normal proliferation to PHA, but completely defective proliferation to immobilized anti-CD3 in the patient (Fig. 1 B). In contrast, the proliferation of T cells from the WAS patient to anti-CD3 was only partially decreased. Addition of IL-2 failed to correct the inability of the patient's T cells to proliferate to anti-CD3 (Fig. 1 B), and induced only modest STAT5 phosphorylation compared with control T cells (Fig. 1 C). In contrast, IL-2 completely corrected the proliferation of WASP-deficient T cells to anti-CD3 (Fig. 1 B) and caused normal STAT5 phosphorylation in these cells (Fig. 1 C). Migration toward the C-X-C motif chemokine immune protein-10 (IP-10) was abolished in PHA blasts from the patient at all three concentrations tested (Fig. 1 D). WASP-deficient PHA blasts responded to the highest concentration of IP-10 tested, but not to the lower two concentrations. Expression of the IP-10 receptor CXCR3 was lower in the patient's T cells (Fig. 1 E), and may have contributed to their failure to migrate toward IP-10. Analysis of cytolytic activity of freshly isolated NK cells from the patient was precluded by the amount of blood that could be drawn. To circumvent this limitation, NK cells were expanded by stimulating T cell–depleted PBMCs from patient and a control with PHA and rIL-2 in the presence of feeder cells (Castriconi et al., 2007). The resulting cell lines contained >90% $CD56^+$ NK cells, which expressed comparable levels of CD56 on their surface. However, expression of NKp30, NKp46, and NKG2D, all of which are implicated in NK cytotoxicity, were reduced on the patient's cells (Fig. 1 F). Analysis of cytolytic activity against LCL 721.221 target cells demonstrated a drastic reduction in the functional activity of the patient's NK cell line compared with that from control (Fig. 1 G). Previous studies have shown impaired cytotoxicity of freshly isolated NK cells from WAS patients (Gismondi et al., 2004). We have been unable to derive NK cell lines from the WAS patient for direct comparison with the NK cell line from our patient.

WIPF1 is mutated in the patient

Although the *WAS* gene is located on the X-chromosome, several cases of WAS in females caused by extreme lyonization or biallelic *WAS* mutations have been described

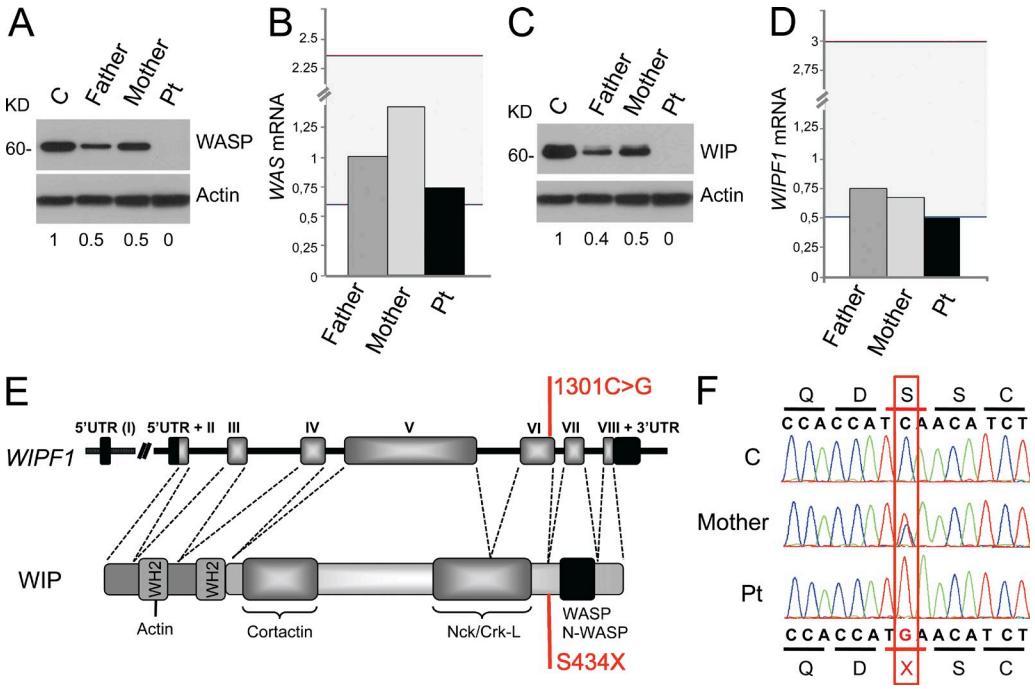

Figure 2. WIP is mutated in the patient. (A and C) Western blot analysis of WASP (A) and WIP (C) in lysates of PHA T cell blasts. Numbers at the bottom indicate densitometric quantification corrected for the actin signal. Data are representative of two experiments. (B and D) qPCR analysis of mRNA expression of *WAS* (B) and *WIPF1* (D) in PHA T blasts, relative to the housekeeping gene *GAPDH*, normalized to 1 for the mean of 25 controls. The gray area indicates the range for the 25 controls. Data are representative of three experiments conducted on triplicates. (E) Genomic organization of *WIPF1* (top) and protein structure (bottom) of WIP showing the localization of the mutation and the resulting amino acidic change (in red) from Serine to a premature termination codon (S434X). The genomic organization shows coding exons, indicated with Roman numbers, and 5′ and 3′ untranslated regions (UTR). Protein structure includes known WIP-interacting protein domains and WASP homology 2 (WH2). (F) Electropherogram depicting the homozygous c.1301C>G mutation in exon 6 in the patient and the presence of the same mutation in the heterozygous state in the mother.

Published January 9, 2012

(Lutskiy et al., 2002; Proust et al., 2005). Western blot analysis revealed no detectable WASP in lysates of the patient's PHA T blasts (Fig. 2 A). WASP expression in the PHA T blasts from both parents was reduced to ∼50% of normal as assessed by Western blot compared with the mean of four controls (Fig. 2 A and not depicted). Similar results were obtained by flow cytometric analysis of PBMCs from the patient and her parents (unpublished data). The levels of *WAS* mRNA in PHA T blasts from the patient and her parents were within the normal range of 25 controls (Fig. 2 B). Sequencing of the *WAS* gene in the patient revealed no mutations.

The absence of WASP expression in the patient's cells, despite normal *WAS* sequence and mRNA expression level, suggested that WASP was being degraded. Because WIP stabilizes WASP, we examined its expression. Western blot analysis of PHA T blasts from the patient revealed no detectable WIP (Fig. 2 C). WIP expression in the PHA T blasts from both parents was reduced to ∼50% of normal (n = 4). These results were confirmed by flow cytometric analysis of PBMCs from the patient and her parents (unpublished data).

Quantitative PCR analysis revealed that the *WIPF1* mRNA level in the patient's PHA T blasts was at the lowest limit of the normal range of 25 controls (Fig. 2 D). *WIPF1* mRNA levels in the parents were in the lower range of normal. Sequencing of genomic DNA revealed that the patient had a homozygous point mutation c.1301C>G in exon 6 of the *WIPF1* gene located on chromosome 2 (Fig. 2, E and F). This mutation results in a change from serine to premature termination in codon 434 (S434X), situated immediately upstream of the region encoding the WASP-binding domain of WIP (451–485 aa; Ramesh et al., 1997). Both parents were heterozygous for the c.1301C>G substitution, confirming the autosomal recessive inheritance of the mutation.

Expression of WIP in the patient's cells corrects the defect in WASP expression

We examined whether expression of human WIP (hWIP) in the patient's cells corrects their defective WASP expression. PHA T blasts from the patient and a control were transfected with vectors expressing EGFP-hWIP fusion protein or EGFP alone, and their content of WIP and WASP was determined by FACS analysis of intracellular staining. As expected, introduction of EGFP-hWIP, but not EGFP, in the patient's T cells resulted in WIP expression, as indicated by the detection of WIP$^+$ cells in the EGFP$^+$ gate (Fig. 3 A). More importantly, introduction of EGFP-hWIP, but not EGFP, in the patient's T cells resulted in increased WASP expression by EGFP$^+$ cells (Fig. 3 B). WASP expression in the EGFP-hWIP–transfected cells from the patient correlated with WIP expression (Fig. 3 C). These findings indicate that the absence of WIP in the patient's T cells resulted in WASP instability and degradation. Because the patient was transplanted at 4.5 mo of age and because of the limited amounts of blood we could obtain pretransplant, we were not able to examine whether transduction of WIP in the patients T cells would restore their function or examine the cortical actin meshwork in the patient's T cells, which is severely attenuated in WIP$^{-/-}$ but not WASP$^{-/-}$ mice (Antón et al., 2002).

Several of the clinical characteristics and laboratory findings in the patient resemble those found in WAS. They include recurrent infections, eczematous skin rash, thrombocytopenia, T cell lymphopenia affecting

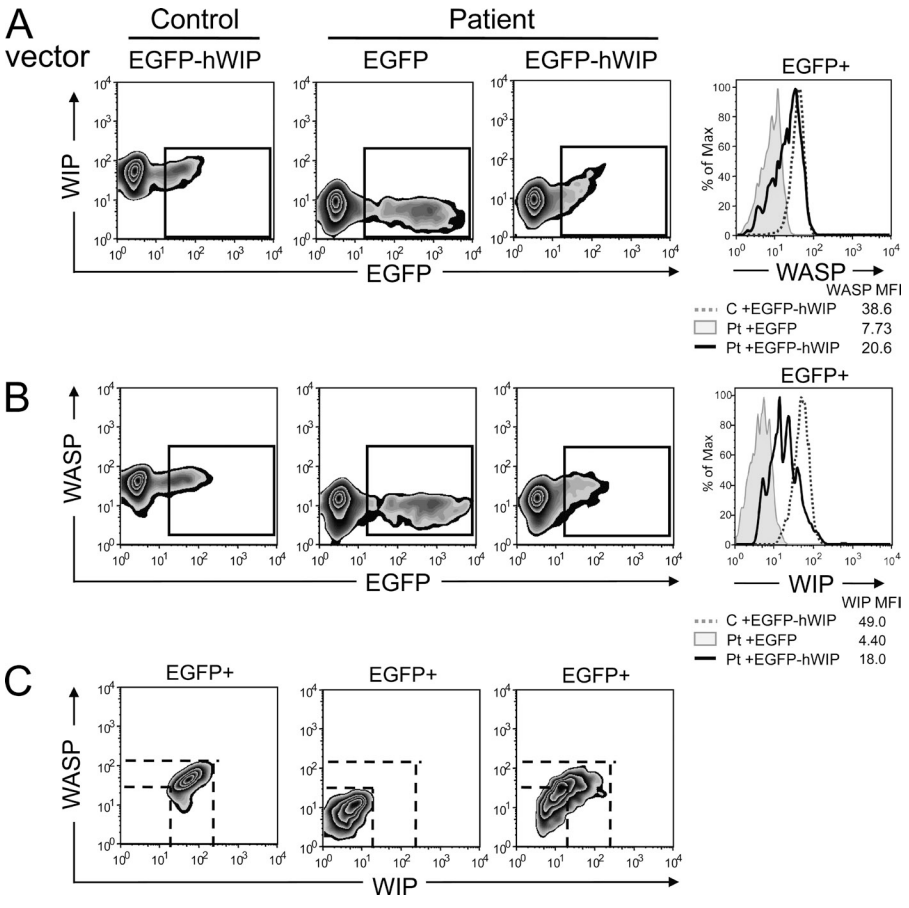

Figure 3. Introduction of WIP restores WASP levels in the patient T cells. (A and B) Two-color FACS analysis of expression of WIP (A) and WASP (B) versus EGFP in PHA T cell blasts transfected with vectors encoding EGFP-hWIP for patient and control and with EGFP alone for the patient. Histograms depicting WIP and WASP expression in gated EGFP$^+$ cells are shown in the right panels. (C) Two-color FACS analysis of WASP versus WIP expression in gated EGFP$^+$ cells. Data are representative of two different analyses.

Published January 9, 2012

$CD8^+$ lymphocytes more severely, impaired T cell proliferation to immobilized anti-CD3, defective T cell chemotaxis, and increased NK cell number but decreased NK cell function. In addition, the patient displayed immune abnormalities that are observed in WIP-deficient mice, but not in WAS patients or WASP-deficient mice. They include complete failure to proliferate to TCR ligation with anti-CD3, impaired response of T cells to IL-2, and complete abrogation of T cell chemotaxis (Fig. 1; Haddad et al., 2001; Gallego et al., 2006; Le Bras et al., 2009). In contrast to WAS patients, platelet volume was normal in the patient, like in WIP-deficient mice (Curcio et al., 2007). However, we hesitate to draw a firm conclusion on platelet size in human WIP deficiency based on a single patient.

Despite undetectable WASP in the patient, no mutations were detected in the coding region of the *WAS* gene and *WAS* mRNA levels were normal, findings strongly indicative of WASP instability. WIP, which is critical for the stability of WASP, was undetectable in the patient's cells, and a homozygous mutation that introduces a premature stop codon in the *WIPF1* coding sequence was identified in the patient. The same mutation was found in the heterozygous state in both parents, indicating that WIP deficiency was inherited as an autosomal recessive trait. This is consistent with an older sibling having died from a similar condition. The fact that both parents showed reduced levels of WIP, to approximately half of normal, suggests a gene dose effect. The correspondingly reduced WASP level in the parents suggests that WIP tightly regulates WASP levels. We have observed a similar reduction of WASP levels in mice heterozygous for a WIP-null allele (unpublished data). Importantly, we demonstrated that reconstitution of the patient's T cells with WIP restores WASP levels, indicating that loss of WIP expression was the cause of WASP instability in the patient's cells.

Collectively, the data indicate that WIP deficiency is responsible for the immune dysfunction in the patient. Based on our findings, WAS cannot be diagnosed solely on the basis of lack of WASP expression, but requires sequence analysis of *WAS*. WIP deficiency should be suspected in patients with features of WAS in whom *WAS* sequence and mRNA levels are normal, and the diagnosis should be confirmed by sequencing *WIPF1*.

MATERIALS AND METHODS

Cell purification and culture. Patient's samples were obtained upon informed consent by the local Institution Review Board and in respect to the Helsinki declaration. Human studies were approved by the Ethical Committee of Azienda Ospedaliera Spedali Civili, Brescia. Isolation of peripheral blood mononuclear cells (PBMCs) and of specific cell populations and establishment of cell lines were performed as follow: to obtain PHA T blasts, PBMCs were stimulated with 5 µg/ml PHA (Sigma-Aldrich) and 600 U/ml rIL-2 (Cairon-Novartis) in RPMI medium containing 10% FCS, 1% L-glutamine, and 1X antibiotics (EuroClone). To generate NK cell lines, NK cells were purified by NK cell separation cocktail (Rosette Sep; StemCell Technologies). The purity of NK cells was >96% as assessed by flow cytometric analysis of cells stained with a mixture of CD56-PC5 and CD3-FITC (Beckman Coulter). CD3 contamination was <1%. Purified NK cells were cultured on irradiated feeder cells in the presence of 100 U/ml of rIL-2 and 5 µg/ml of PHA (Invitrogen) to obtain activated polyclonal NK cell populations. Activated polyclonal NK cells were maintained in complete RPMI medium containing 1,200 U/ml of rIL-2.

Molecular genetic analyses. Genomic DNA was isolated using the automatic DNA extractor Maxwell 16 (Promega). Sequencing of genomic DNA corresponding to the coding regions of *WAS* (ENSG00000015285) and *WIPF1* (ENSG00000115935) genes was performed by direct sequencing after PCR amplification of exons with flanking intronic regions. Primers and conditions are reported in Table S2.

Total RNA was isolated from PBMCs using the RNeasy Mini kit (QIAGEN) and transcribed into complementary DNA (cDNA). Quantitative PCR experiments were performed by reverse transcription of 200 ng of DNase-treated total RNA to synthesize the first strand of cDNA by the GeneAmp RNA PCR kit (Applied Biosystems). Analysis of *WASP*, *WIPF1*, and *GAPDH* gene expression was assessed by RealTime PCR using Assays-on-Demand products and TaqMan Master Mix from Applied Biosystems. The level of expression was normalized using *GAPDH* as a reference.

Immunoblotting. Cell lysates from PHA T blasts were prepared and 10 µg protein were loaded on a 10% SDS-PAGE and transferred onto a polyvinylidene fluoride membrane (GE Healthcare). Specific proteins were detected using mouse IgG1 anti-WIP mAb (3D10; Koduru et al., 2007), mouse IgG2a anti-WASP mAb 5A5 (BD), and mouse anti-actin mAb (US Biological).

Flow cytometry. Flow cytometry for surface and intracellular proteins was performed on 100 µl of whole blood or isolated cells (1.5×10^6) resuspended in 100 µl of the appropriate medium. To assess WASP and WIP expression, cells were treated with the Fix and Perm kit (Invitrogen) for FACS analysis. Cells were stained with mouse IgG1 anti WIP (3D10; Koduru et al., 2007) and mouse IgG2a anti-WASP (5A5; BD), followed by anti IgG1PE and biotinylated anti–IgG2a-streptavidinPECy5, respectively. Acquisition was performed using a FACSCalibur (BD), and data were analyzed with FlowJo Software v7.5 (Tree Star).

Standard flow cytometric methods were also used for CFSE assay. CFSE labeling (100 nM) was performed in PBS for 6 min at 37°C. Cells were then washed twice in RPMI 10% FCS. Cells were cultured for 96 h in the absence of stimulation or stimulated with anti-CD3 (clone OKT3, 100 ng/ml) and anti–human CD28 (1 µg/ml) or PHA (5 µg/ml) and then analyzed for CFSE dilution.

For the characterization of NK cells, the following mAbs, which were produced in our laboratories, were used in this study: BAB281 (IgG1anti-NKp46), AZ20 (IgG1, anti-NKp30), c218 (IgG1, anti-CD56), BAT221 (IgG1, anti-NKG2D), and 289 (IgG2a, anti-CD3). For cytofluorimetric analysis, cells were stained with mAb PE-conjugated isotype-specific goat anti–mouse secondary antibody (SouthernBiotech). Cell acquisition was performed on a FACScan flow cytometer (BD), and data were analyzed using the CellQuest software (BD).

Lymphocyte functional analysis. Analysis of STAT5 phosphorylation in T cells in response to IL-2 was assessed by flow cytometry: 100 µl of whole blood was incubated with or without 100 ng/ml rIL-2 (Proleukin-Chiron) for 10 min at 37°C. Activation was stopped using Lyse/Fix buffer (BD). After washing, the samples were permeabilized by PBIII Buffer (BD) for 30 min on ice and incubated with anti–phospho-STAT5 (Y694)-PE and CD3-FITC, or with isotype-matched mAb PE (BD) for 30 min at room temperature. Samples were then washed and resuspended in 200 µl of BD CellFix and analyzed with FACSCalibur instrument (BD). To analyze NK cytolytic activity, PBMCs were depleted of T cells and expanded in vitro with rIL-2, resulting in highly enriched (>95%) $CD56^+$ NK lymphocytes, which were tested for cytolytic activity against the NK-susceptible tumor target cell line LCL 721.221 in a 4-h ^{51}Cr-release assay. Target cells were used at 5×10^3 cells/well with final E/T ratios of 6:1 and 3:1.

Chemotaxis assay. In vitro chemotaxis of PHA T blasts toward IP-10 was examined using a standard Transwell chamber assay: a total of 3×10^5 PHA T blasts were added to the upper chamber of a plate 6.5 mm in diameter with a pore size of 5 μm (Costar). 600 μl of RPMI 1640 with 0.1% FCS was added to the bottom chamber with or without IP10 (250, 500, and 1,000 ng/ml; PeproTech). After 2 h at 37°C, cells that migrated to the lower chamber were collected and counted. The experiment was performed in duplicates. Expression of the IP-10 receptor CXCR3 was examined by FACS using a mouse anti–CXCR3-FITC mAb (R&D Systems).

WIP reconstitution experiment. hWIP cDNA was generated from normal PBMCs by RT-PCR and cloned into the BglII–PstI cloning sites of the pAC-EGFP vector. Confirmation of the WT WIP sequence and its in-frame insertion in the vector was obtained by direct sequencing. PHA T blasts were transfected using the Amaxa nucleofection technology (Lonza) according to the manufacturer's protocol, which is optimized for stimulated human T cells. In brief, $2–3 \times 10^6$ cell suspension was mixed with 1 $\mu g/10^6$ cell of both mock and hWIP-containing plasmid DNA, transfected using the T-020 program, then cultured for 48 h in the growth medium. Mock- and hWIP-transfected cells were treated with the Fix/Perm kit (Invitrogen) for FACS analysis. Cells were stained with mouse IgG1 anti WIP (3D10) and mouse IgG2a anti WASP (5A5), followed by anti–IgG1-PE and biotinylated anti–IgG2a-streptavidin-PECy5, respectively. Acquisition was performed using a FACSCalibur (BD), and analysis was performed by FlowJo software (Tree Star). Transfected PHA-T cells were evaluated for WASP and WIP expression level gating on $EGFP^+$ cells.

Online supplemental material. Table S1 provides the Laboratory data of the patient at 3 wk of age. Table S2 provides the list of the primers used for the amplification of the *WIPF1* gene. Online supplemental material is available at http://www.jem.org/cgi/content/full/jem.20110896/DC1.

This work was supported by Fondazione 'A. Nocivelli' to S. Giliani; United States Public Health Services grant 5PO1HL059561 to S. Giliani, L.D. Notarangelo, and R.S. Geha; Fondazione C. Golgi to A. Plebani; the Jeffrey Modell Foundation; and the Perkin fund. D. Vairo is recipient of a Rotary Brescia fellowship.

The authors have no conflicting financial interests.

Submitted: 4 May 2011
Accepted: 7 December 2011

REFERENCES

Antón, I.M., M.A. de la Fuente, T.N. Sims, S. Freeman, N. Ramesh, J.H. Hartwig, M.L. Dustin, and R.S. Geha. 2002. WIP deficiency reveals a differential role for WIP and the actin cytoskeleton in T and B cell activation. *Immunity*. 16:193–204. http://dx.doi.org/10.1016/S1074-7613(02)00268-6

Castriconi, R., A. Dondero, M. Cilli, E. Ognio, A. Pezzolo, B. De Giovanni, C. Gambini, V. Pistoia, L. Moretta, A. Moretta, and M.V. Corrias. 2007. Human NK cell infusions prolong survival of metastatic human neuroblastoma-bearing NOD/scid mice. *Cancer Immunol. Immunother.* 56:1733–1742. http://dx.doi.org/10.1007/s00262-007-0317-0

Curcio, C., T. Pannellini, S. Lanzardo, G. Forni, P. Musiani, and I.M. Antón. 2007. WIP null mice display a progressive immunological disorder that resembles Wiskott-Aldrich syndrome. *J. Pathol.* 211:67–75. http://dx.doi.org/10.1002/path.2088

de la Fuente, M.A., Y. Sasahara, M. Calamito, I.M. Antón, A. Elkhal, M.D. Gallego, K. Suresh, K. Siminovitch, H.D. Ochs, K.C. Anderson, et al. 2007. WIP is a chaperone for Wiskott-Aldrich syndrome protein (WASP). *Proc. Natl. Acad. Sci. USA*. 104:926–931. http://dx.doi.org/10.1073/pnas.0610275104

Gallego, M.D., M.A. de la Fuente, I.M. Anton, S. Snapper, R. Fuhlbrigge, and R.S. Geha. 2006. WIP and WASP play complementary roles in T cell homing and chemotaxis to SDF-1alpha. *Int. Immunol.* 18:221–232. http://dx.doi.org/10.1093/intimm/dxh310

Gismondi, A., L. Cifaldi, C. Mazza, S. Giliani, S. Parolini, S. Morrone, J. Jacobelli, E. Bandiera, L. Notarangelo, and A. Santoni. 2004. Impaired natural and CD16-mediated NK cell cytotoxicity in patients with WAS and XLT: ability of IL-2 to correct NK cell functional defect. *Blood*. 104:436–443. http://dx.doi.org/10.1182/blood-2003-07-2621

Haddad, E., J.L. Zugaza, F. Louache, N. Debili, C. Crouin, K. Schwarz, A. Fischer, W. Vainchenker, and J. Bertoglio. 2001. The interaction between Cdc42 and WASP is required for SDF-1-induced T-lymphocyte chemotaxis. *Blood*. 97:33–38. http://dx.doi.org/10.1182/blood.V97.1.33

Koduru, S., M. Massaad, C. Wilbur, L. Kumar, R. Geha, and N. Ramesh. 2007. A novel anti-WIP monoclonal antibody detects an isoform of WIP that lacks the WASP binding domain. *Biochem. Biophys. Res. Commun.* 353:875–881. http://dx.doi.org/10.1016/j.bbrc.2006.12.079

Le Bras, S., M. Massaad, S. Koduru, L. Kumar, M.K. Oyoshi, J. Hartwig, and R.S. Geha. 2009. WIP is critical for T cell responsiveness to IL-2. *Proc. Natl. Acad. Sci. USA*. 106:7519–7524. http://dx.doi.org/10.1073/pnas.0806410106

Lutskiy, M.I., Y. Sasahara, D.M. Kenney, F.S. Rosen, and E. Remold-O'Donnell. 2002. Wiskott-Aldrich syndrome in a female. *Blood*. 100:2763–2768. http://dx.doi.org/10.1182/blood-2002-02-0388

Orange, J.S., N. Ramesh, E. Remold-O'Donnell, Y. Sasahara, L. Koopman, M. Byrne, F.A. Bonilla, F.S. Rosen, R.S. Geha, and J.L. Strominger. 2002. Wiskott-Aldrich syndrome protein is required for NK cell cytotoxicity and colocalizes with actin to NK cell-activating immunologic synapses. *Proc. Natl. Acad. Sci. USA*. 99:11351–11356. http://dx.doi.org/10.1073/pnas.162376099

Proust, A., B. Guillet, I. Pellier, P. Rachieru, C. Hoarau, S. Claeyssens, C. Léonard, S. Charrier, W. Vainchenker, G. Tchernia, and J. Delaunay. 2005. Recurrent V75M mutation within the Wiskott-Aldrich syndrome protein: description of a homozygous female patient. *Eur. J. Haematol.* 75:54–59. http://dx.doi.org/10.1111/j.1600-0609.2005.00415.x

Ramesh, N., I.M. Antón, J.H. Hartwig, and R.S. Geha. 1997. WIP, a protein associated with wiskott-aldrich syndrome protein, induces actin polymerization and redistribution in lymphoid cells. *Proc. Natl. Acad. Sci. USA*. 94:14671–14676. http://dx.doi.org/10.1073/pnas.94.26.14671

Stabile, H., C. Carlino, C. Mazza, S. Giliani, S. Morrone, L.D. Notarangelo, L.D. Notarangelo, A. Santoni, and A. Gismondi. 2010. Impaired NK-cell migration in WAS/XLT patients: role of Cdc42/WASp pathway in the control of chemokine-induced beta2 integrin high-affinity state. *Blood*. 115:2818–2826. http://dx.doi.org/10.1182/blood-2009-07-235804

Thrasher, A.J., and S.O. Burns. 2010. WASP: a key immunological multitasker. *Nat. Rev. Immunol.* 10:182–192. http://dx.doi.org/10.1038/nri2724